

Article

Genesis of Significance of Carbonated Thermal Water Springs in Xining Basin, China

Yude Lei ^{1,2,3} , Zhen Zhao ^{1,2,3}, Baojian Zhang ^{4,5,*}, Xianchun Tang ^{4,5}, Yinfei Luo ^{1,2,3}, Guiling Wang ^{4,5,*}, Jun Gao ^{4,5,*} and Dailei Zhang ^{4,5}

¹ Key Laboratory of Geo-Environment Qinghai Province, Xining 810007, China

² Environmental Geological Prospecting Bureau of Qinghai Province, Xining 810007, China

³ Qinghai 906 Engineering Survey and Design Institute Co., Ltd., Xining 810007, China

⁴ Chinese Academy of Geological Sciences, Deep Earth Science and Exploration Technology Laboratory, Beijing 100037, China

⁵ Technology Innovation Center of Geothermal and Hot Dry Rock Exploration and Development, Ministry of Natural Resources, Shijiazhuang 050061, China

* Correspondence: zbssddk@126.com (B.Z.); guilingw@163.com (G.W.); gjun@cags.ac.cn (J.G.)

Abstract: There are 30 carbonate hot springs in Yaoshuitan geothermal field, Xining Basin, China, with a temperature of 18~41.5 °C; and there are 10 carbonate hot springs in Qijiachuan geothermal field, with a temperature of 10~19.5 °C. Both geothermal fields are carbonate hot springs containing large amounts of CO₂ gas. In order to reveal the origin of the carbonated hot springs in Yaoshuitan and Qijiachuan of Xining Basin, this paper offers a comprehensive study of the regional deep geology, tectonic setting, total analysis of carbonated hot springs, $\delta^2\text{H}$, $\delta^{18}\text{O}$, $\delta^{13}\text{C}$ isotopes, main gas composition, and geochemical characteristics of travertine dating, travertine $\delta^{13}\text{C}$, and rare earth elements. The geological process of carbonated hot spring formation and the evolution of H⁺ content from deep to shallow is revealed, and the genetic mechanism of the carbonated hot spring in Xining Basin is systematically summarized. The results show that: (1) The characteristics of $\delta^2\text{H}$ and $\delta^{18}\text{O}$ isotopes indicate that the recharge source of carbonated thermal water springs in Xining Basin is mainly atmospheric precipitation. The age of carbonated thermal water springs at ¹⁴C is more than 20 ka, indicating that some of them may come from deep fluid (gas) sources. The R/Ra in carbonated thermal water springs is mostly less than 1, indicating that the helium in geothermal water is mainly crustal source helium, and there is no deep mantle source material. (2) The Piper three-plot indicates that the direction of groundwater evolution from the recharge area at the edge of Xining Basin to Yaoshuitan and Qijiachuan carbonated thermal water spring area near the edge of the basin is opposite to the normal path of groundwater evolution in the basin, which is due to the large amount of CO₂ gas mixed in the deep fault along the northern margin of Laji Mountain. The ratio of (Ca²⁺ + Mg²⁺) and (HCO₃⁻ + SO₄²⁻) in the Potan and Qijiachuan carbonated thermal water springs is close to 1, and the ratio of (Na⁺ + K⁺)/HCO₃⁻ is less than 1. It indicates that the chemical composition of the Yaoshuitan carbonated thermal water spring and the Qijiachuan carbonated thermal water spring in Xining Basin is dominated by the dissolution of calcite, dolomite, and gypsum in deep carbonate reservoirs, supplemented by the dissolution of silicate minerals. The relationship between the volume fraction of CO₂ and the $\delta^{13}\text{C}$ value of carbon isotope of CO₂ indicates that the source of CO₂ is inorganic, which is mainly formed by metamorphism and decomposition of deep carbonate and marble. The $\delta\text{Eu} < 1$ and $\delta\text{Ce} > 1$ of the rare earth elements in the calcium center of the carbonated thermal water springs indicate that the groundwater supplying the travertine material has been in the acidic environment receiving CO₂ from the deep crust for a long time. (3) A series of tectonic activities, such as late collision and post-collision between the Indian and Eurasian plates, has led to the uplift, asthenosphere upwelling, and thermal invasion of the northern Tibetan Plateau and other deep dynamic processes. The deep faults in the northern margin of the Laji Mountain and other deep faults with obvious neotectonic activity have provided channels for the up-invasion of deep thermal materials, and local geothermal anomalies were formed near the deep faults. The hidden carbonate rocks and silicate rocks with large thickness undergo thermal metamorphism under high temperature



Citation: Lei, Y.; Zhao, Z.; Zhang, B.; Tang, X.; Luo, Y.; Wang, G.; Gao, J.; Zhang, D. Genesis of Significance of Carbonated Thermal Water Springs in Xining Basin, China. *Water* **2022**, *14*, 4058. <https://doi.org/10.3390/w14244058>

Academic Editor: Elias Dimitriou

Received: 26 September 2022

Accepted: 9 December 2022

Published: 12 December 2022

Publisher's Note: MDPI stays neutral with regard to jurisdictional claims in published maps and institutional affiliations.



Copyright: © 2022 by the authors. Licensee MDPI, Basel, Switzerland. This article is an open access article distributed under the terms and conditions of the Creative Commons Attribution (CC BY) license (<https://creativecommons.org/licenses/by/4.0/>).

and high pressure in the deep geothermal anomaly area and form a large amount of CO₂, which is dissolved in water and enhances the acidity of water. At the same time, the dissolution reaction of acidic water to carbonate rocks consumes H⁺, which keeps the carbonated thermal water spring weakly acidic. (4) The composition of travertine in carbonated thermal water springs is dominated by calcite, indicating that travertine may be formed in a deep geological environment with a temperature of 150~200 °C, indicating that there are abnormal heat sources in shallow carbonate strata with a burial depth of 3000~4000 m. The abnormal heat source may be caused by the deep fault in the northern margin of Laji Mountain, as well as other deep and large faults channeled in the deep crust and mantle heat source, indicating that the deep fault in the northern margin of Laji Mountain has an obvious heat-controlling effect, and there is a good prospect of geothermal resources exploration near the fault.

Keywords: carbonated thermal water springs; genetic mechanism; deep fault in the northern margin of Laji Mountain; heat control; Xining Basin

1. Introduction

The Earth's deep-source gas emissions [1] and their environmental effects [2,3] have been gradually attracting the attention of geologists. Most of the carbon in the Earth system occurs in the Earth's interior [4], and is mainly released from the Earth's interior to the atmosphere in the form of CO₂ through different tectonic processes [5–7]. In recent years, studies on deep-source gas emissions, including CO₂ from volcanic–geothermal systems, as well as deep faults and their causes, have increased [8]. The CO₂ degassing flux and genesis of the Lassa terrane–Yadong rift volcanic–geothermal system in southern Tibet have been studied [9,10].

Springs with carbonated geothermal water have a special type of geothermal water. In both neotectonic active areas and modern volcanic active areas, a large amount of deep-source CO₂ is mainly released outward through geothermal water as a carrier, and only a small amount is released via geothermal springs in the form of CO₂ gas. This is because CO₂ is easily dissolved in water; in particular, under conditions of deep, high confining pressure, CO₂ usually migrates and is released with geothermal water [11]. It can be seen that carbonated geothermal springs provide an important outlet for CO₂ emissions in the Earth. Current studies on carbonated geothermal springs mainly focus on the relationship between earthquakes and the distribution of carbonated thermal water springs [11,12]. Research on carbonated thermal water springs and their formation mechanisms has increased in recent years, which indicates that the study of fluid earth is garnering increasing attention. Chris et al. (2018) studied the Valles Caldera geothermal system in the Nacimiento Mountains and pointed out that deep circulation along faults and mixing of different aquifers are responsible for the formation of carbonated waters springs [13]. Nisi et al. (2019) studied the CO₂-rich fluid geochemistry in the Campo de Calatrava volcanic area in Spain, and pointed out that the interaction between shallow water and deep carbon dioxide caused a decrease in pH [14]. Italiano et al. (2016) studied the geochemical characteristics and genesis of dissolved gasses in the eastern Carpathian Mountains, Transylvania Basin, Romania, and pointed out that in addition to obvious atmospheric gas sources, volcanic and crustal gas sources provide materials for circulating groundwater [15]. Shvartsev et al. (2017) analyzed the origin and evolution of the high pCO₂ groundwater in the Mukhen geothermal springs in the Russian Far East [16]. Kharaka et al. (2018), through an experiment on the reaction between groundwater and CO₂, showed that the leakage of CO₂ into groundwater increased acidity, which increased the content of Fe and other metals in groundwater [17]. Zhang et al. (2005) and Li et al. (2018) studied the genesis of carbonated thermal water spring CO₂ in the Hengjing area of southern Jiangxi Province and the Heyuan fault zone of Guangdong Province, respectively, and pointed out that the carbonated thermal water spring CO₂ in Hengjing area of southern Jiangxi Province is

mainly deep mantle-derived inorganic gas related to deep and large fault activities [18]. The carbonated thermal water spring CO₂ in the Heyuan fault zone is of mixed origin, from mantle source and metamorphism, mainly the latter [19]. Zhou et al. (2020) studied the geochemical characteristics of hot spring gas in the Jinshajiang–Honghe fault zone and pointed out that CO₂ gas in geothermal springs mainly came from limestone cracking [20]. Yu et al. (2022) studied the geochemical characteristics and geological significance of geothermal spring gas in the northern Yadong Rift Valley of the Qinghai Tibet Plateau, and pointed out that the thermal decomposition of carbonate rocks was the main source of CO₂ [21]. Walter et al. (2020) studied CO₂ released into the atmosphere by geothermal springs in the Sperchios basin, northern Greece, and the resulting travertine deposition [22]. Wang et al. (2020) pointed out that due to the high pCO₂ values (10–3.5 atm) in geothermal spring water and the escape of CO₂ from water after the spring water emerged from the surface, CaCO₃ was deposited to form travertine [23]. Ta et al. (2020) discussed the evolution and source of major ions in triassic carbonate hot springs in Chongqing. These related studies revealed the source and migration of CO₂ gas in hot springs from different perspectives [24].

Xining Basin is located in the northeast of Qinghai Province. The study of Xining geothermals began in the 1960s. In recent years, due to the increasing degree of geothermal development and utilization, Xining geothermal research has gradually attracted scholarly attention. There has been significant research data collected on the geothermal geology of Xining Basin that mainly focus on geothermal field characteristics [25] and causes [26,27], water chemistry characteristics and causes [28,29], a thermal storage conceptual model [30], etc. The Yaoshuitan geothermal spring in Xining Basin has been developed and utilized for hundreds of years, and is called a ‘sacred spring’ because of its obvious therapeutic effects. In 1986, the Qinghai New Energy Research Institute carried out an evaluation of drinking mineral water of the Yaoshuitan spring group, and the free CO₂ content of two springs in Yaoshuitan spring group was found to be as high as 718.5–884.4 mg/L. At the end of 2002, the China Geological Survey discovered a high CO₂ gas–water mixed high-pressure artesian thermal well in the terrace of Qijiachuan in Pingan County, Qinghai Province. In addition, in 2016, when China Railway First Survey and Design Institute Group Co., Ltd. constructed the exploration hole of the Xining–Chengdu Railway Haidongnanshan Tunnel (about 5 km from the Qijiachuan), gas at a depth of ~5 m and a strong whistling sound was drilled out. The gas had no abnormal smell. It took 11 days to complete the drilling and plugging, and there was no attenuation. After borehole sampling and analysis, the gas composition was mainly CO₂ [31]. It was proved that there are carbonated thermal water springs and CO₂ gas reservoirs in parts of Xining Basin. Zheng et al. (2016) studied the accumulation model of the CO₂ gas reservoir in the Pingan area of Qinghai Province [32]. These exploration results prove that there are carbonated thermal water springs and CO₂ gas reservoirs in some parts of Xining Basin, and they are weakly acidic. Although the formation of CO₂ gas reservoirs in Xining Basin has been preliminarily revealed, the formation of carbonated thermal water springs and the reason why carbonated thermal water springs are weakly acidic have not been systematically studied.

In this study, detailed hydrochemistry and isotope studies were conducted on carbonated thermal water springs, ordinary geothermal water, and gas samples collected from the Xining Basin. The purpose of this study is: (i) to determine the origin and hydrogeochemical formation process of carbonated thermal water springs, and to preliminarily analyze the heat source; (ii) to analyze the origin of CO₂ in carbonated thermal water springs and the changes of H⁺ content during its migration from the deep to the surface; (iii) to reveal the relationship between the formation of carbonated thermal water springs and the deep fault in the northern margin of Laji Mountain, judge the heat control function of the deep fault in the northern margin of Laji Mountain, and deepen the understanding of the occurrence law of geothermal resources in this area.

2. Geological Background

2.1. Regional Geological Features

Xining Basin is located in the Middle Qilian island arc uplift zone, which is a Mesozoic–Cenozoic faulted basin. The formation of Xining Basin is restricted by the deep faults of the north margin of Laji Mountain in the south and the deep faults of Daban Mountain in the north (Figure 1). Xining Basin comprises cap rocks and a basement. The cap rocks are Mesozoic and Cenozoic stratigraphic strata, which are mainly characterized by the large thickness of sedimentary rocks, basically horizontal in occurrence and with a large distribution range. The basement structure mainly includes three-level structural units, such as the Laoyeshan uplift, western slope, Shuangshuwan depression, Dabaozi–Xining uplift, Zongzhai depression, and Xiaoxia uplift. Xining Basin has an obvious double-layer structure, and its basement is a dome structure composed of Proterozoic. Above the basement are the Triassic, continental Jurassic, fluvial–lacustrine Cretaceous, inland lacustrine Paleogene, piedmont alluvial–proluvial facies Neogene and Quaternary, and contact with false conformity or angle unconformity. The basement morphology of Xining Basin is not only uneven, but generally shows the characteristics of surrounding elevation and descending to the middle. In the south–north tectonic profile, Xining Basin also has the geothermal tectonic background of deep thermal uplift, extrusion above the neutral tectonic plane, the southern and northern orogenic belts thrust toward the basin, and peristaltic expansion under the ‘pull-down and up-pressure’.

In the north of Xining Basin, there are the Daban Mountains with an altitude of 4000–6000 m, and in the south, there is Laji Mountain with an altitude of more than 4000 m. Under the action of regional principal compressive stress of NEE, geological units on both sides of Xining Basin thrust toward the middle, resulting in fold deformation and fault activity of the basin. The basin edge fault zones that affect the deformation of the basin mainly include the Laji Mountain fault zone, the Dabanshan fault zone, and the Riyueshan fault zone. These faults have obvious activities in the Quaternary period. The Laji Mountain fault zone and the Dabanshan fault zone are characterized by sinistral compression movements, and the Riyueshan fault is mainly characterized by dextral movements. The near north–south faults in the basin are characterized by tension–tensional torsion, high angle, strong activity during the neotectonic period, seismogenesis, water conduction, and heat control.

2.2. Geothermal Geological Characteristics

Xining Basin is a closed confined artesian water basin, and the Mesozoic and Cenozoic clastic sediment particles change from coarse to finer from the edge to center of the basin. In the mountainous area at the edge of the basin, after the groundwater is recharged by atmospheric precipitation and surface water, part of the groundwater runs off along the structural fissures to the center and deep part of the basin, and the deep circulating groundwater is heated in the deep part of the basin to form geothermal water. Because of the continuous circulation movement of groundwater, the deep heat energy is brought to the shallow part, which is discharged in the form of geothermal springs and underground runoff to the outside of the basin. Therefore, Xining Basin is both an artesian water basin and an geothermal water artesian basin [33]. The Meso–Cenozoic fissure-pore-type geothermal reservoir in the interior of the basin and the carbonate fissure-karst-cavity geothermal reservoir in the orogenic belt around the basin are the large-scale and mining-significant thermal storage in Xining Basin. Since the Cenozoic, influenced by the Himalayan orogeny, Xining Basin has experienced strong neotectonic movements, manifested in the resurrection of old faults around the basin and within the basin, and further intensified deep hydrothermal activities, which created a regional geological structure background for the formation of geothermal resources in Xining Basin.

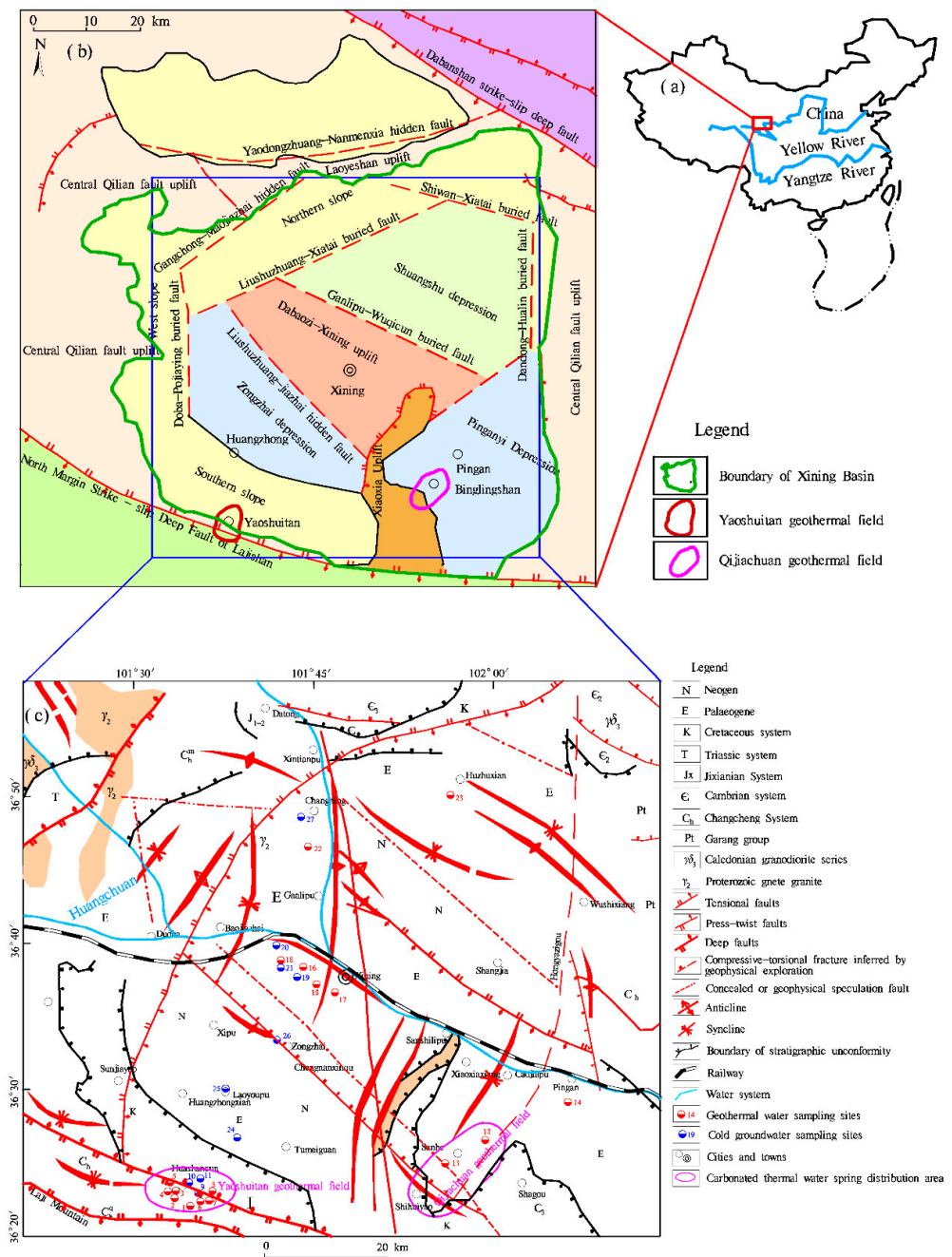


Figure 1. Sketch of geological structure and sampling points and fault location in Xining Basin (slightly modified from reference [27]).

The Yaoshuitan geothermal field is located in the southern margin of Xining Basin. The geomorphology is the northern slope of Laji Mountain and the middle and upper reaches of the Nanchuan Valley. The tectonic location belongs to the northern edge of the Laji Mountain fault zone of the Qilian Mountains’ fold system. The northern margin of Laji Mountain is a deep and large crustal fault zone with a good convective geothermal structure, and its fracture zone is thicker; according to the drilling, there is a fractured zone with a thickness of 1177 m between depths of 103 and 1280 m. Ground mineral water is linearly arranged in the form of springs along the NE direction of the Shuitan fault, forming a large area of marshes and wetlands. The outcrops of the hot field are mainly: Proterozoic gray-white sericite mellite, light gray, black-gray mellite sand–slate; Quaternary alluvial–proluvial sand and gravel; and Quaternary chemical deposits, mainly sinter. Quaternary alluvial–proluvial sand–gravel thickness is 2.0–20.6 m, and its pores are mostly filled with travertine, so it is

cemented sand–gravel. Quaternary chemical deposits (sinter) spread throughout the mineral water distribution area, with a general thickness of 0.8 to 1.5 m, forming a plate-like covering on the ground. The basic aquifers of geothermal wells and geothermal springs are carbonate rocks developed by huge thick fissure karst under the cap rocks. There are 30 natural springs in the mineral water area. The temperature of the springs is 18~41.5 °C, and the free CO₂ content is 6.12~884 mg/L. The geothermal spring water spews out of the surface in the form of a mixture of water and vapor. The pH of geothermal spring water is 6.12~6.55, and it is weakly acidic. The hydrochemical types are mainly HCO₃-Ca·Mg and HCO₃-Ca, and the salinity is 993–1850 mg/L. The cold spring water is slightly alkaline, the pH is 7.10~7.69, and the salinity is generally less than 500 mg/L.

The Qijiachuan geothermal field is located in the Ping'an Depression to the east of Xiaoxia uplift in Xining Basin, and stratigraphic distribution is controlled by the deep fault zone in the north margin of Laji Mountain and Xining Basin. The Upper Proterozoic, Paleozoic, Mesozoic, and Cenozoic strata are all outcropped in the area. The Upper Proterozoic outcropping area is small and sporadic, forming a regional crystalline basement. The Mesozoic and Cenozoic in the area are mainly distributed in the Mesozoic Cretaceous sandstone and conglomerate, and the Cenozoic Paleogene and Neogene mudstone and siltstone. Quaternary aeolian, alluvial, ice-water deposits, and a small amount of travertine deposits are widely distributed, most of which have weak consolidation, loose structures, and varying degrees of thickness. There are 10 geothermal mineral springs, mainly distributed in the NW and NW-trending active fault belts in the piedmont of Laji Mountain, controlled by the geological structure, and there are generally travertine deposits near the spring vent. The geothermal spring water is ejected to the surface as a mixture of water and air, and the partial pressure of CO₂ in the water sample at the spring vent or well head is 59,238.6~71,340 Pa. The pH of geothermal spring water is 6.54~6.63, showing weak acidity. The chemical types of water are mainly HCO₃-SO₄-Ca·Na and HCO₃-Ca·Mg·Na, and the salinity is 2940~5470 mg/L. The higher salinity of geothermal water in this area is due to a larger amount of gypsum salt in the Cretaceous system.

3. Sample Analysis and Research Methods

3.1. Sample Collection and Analysis

In order to determine the origin of carbonated thermal water springs in Xining Basin, according to the occurrence characteristics of geothermal water in Xining Basin, the carbonated thermal water springs in Yaoshuitan geothermal field, Huangzhong County, Qijiachuan geothermal field, Pingan County, and other geothermal water with normal CO₂ content in Xining Basin were analyzed. A total of 29 samples of geothermal water and groundwater were collected; 14 geothermal water samples were analyzed, including 8 Yaoshuitan geothermal spring samples, 2 Qijiachuan geothermal spring samples, and 4 geothermal water from other parts of Xining Basin for comparison. A total of 10 samples of groundwater analysis were analyzed, including 3 samples of Yaoshuitan groundwater, Xining Basin, and 7 samples from other parts of Xining Basin. Isotopic analysis of δ²H and δ¹⁸O was performed on 5 geothermal water samples, including 2 samples of Yaoshuitan geothermal spring, 1 samples of Qijiachuan geothermal spring, and 2 samples of geothermal water from other parts of Xining Basin for comparison (Figure 1c).

The collected samples were sent for analysis at the Key Laboratory of Groundwater Science and Engineering of Land and Resources, Institute of Hydrogeology and Environmental Geology, Chinese Academy of Geological Sciences. During sampling, the water temperature and pH were measured on site by a portable meter. Water samples used for indoor analysis were first filtered with 0.45 μm microporous filter membrane to remove suspended solids, and then loaded into three 100 mL polyethylene bottles that were washed twice with deionized water and dried; water samples needed to fill the sampling bottles to prevent gas from entering. We added 14 mol/L high-grade pure nitric acid to one of the water sample bottles until the pH value of the water sample was lower than 2.0. This water sample was used for routine cation and trace metal element analysis; no reagents were

added to the other two sample bottles for the determination of inorganic anions. Water samples for analysis of $\delta^2\text{H}$ and $\delta^{18}\text{O}$ were stored in brown bottles after filtration in the field. The main detection equipment for total analysis and trace elements were an ICP inductively coupled plasma emission spectrometer (ICAP6300) produced by Thermo Fisher company, and an ion chromatograph (Dionex ICS-1100) produced by Thermo Fisher company, USA. Standard samples were inserted at equal intervals during laboratory analysis to verify the accuracy of analysis results. The absolute error of all samples was not more than 3% by the error analysis of cationic and anion balance. The $\delta^2\text{H}$ and $\delta^{18}\text{O}$ isotopes were measured by a stable isotope ratio mass spectrometer (MAT-253) manufactured by Thermo Fisher, USA. The measured results were expressed as the thousandth difference compared with the Vienna Standard Mean Ocean Water (VSMOW) standard, and the accuracy was $\pm 2.0\%$ and $\pm 0.2\%$, respectively.

3.2. Previous Analysis Data

In order to better reveal the origin of carbonated spring water, this paper used previous analysis and analysis data of geothermal water chemistry, gas, and travertine. These included gas analysis data collected by the Qinghai New Energy Research Institute (1986) from the Yaoshuitan geothermal field, water quality analysis data from the Yaoshuitan geothermal field collected by Li et al. (2017) [28], travertine analysis data from Bingling Mountain in Xining Basin collected by Fu et al. (2019) [34], and groundwater gas analysis data collected from Qijiachuan, Pingan County by the China Railway First Survey and Design Institute Group Co., Ltd., Zheng et al. (2016) [32].

3.3. Research Methods

Firstly, the water source and CO_2 source of carbonated thermal water springs in Xining Basin were identified, and the water-bearing medium and surrounding rock of the formation and occurrence of carbonated thermal water springs were identified through the main components of anions in the carbonated thermal water springs. Then, the main water-rock interactions and chemical reactions during the formation of carbonated thermal water springs were determined by the composition of major anions and travertine deposited in the carbonated thermal water springs. Then, by analyzing the tectonic environment and geological conditions of carbon dioxide formation in the Earth's interior, combined with the tectonic environment of Xining Basin, the most likely formation conditions, formation process, migration path, and accumulation mode of CO_2 in carbonated thermal water springs were summarized, as well as the reason why geothermal springs were acidic. Finally, the temperature range of travertine formation and CO_2 generation was determined by the main mineral composition in the central calcium, and the thermal anomaly was determined by the temperature of deep heat storage, so as to determine whether the deep fault in the northern margin of Lajishan had a thermal control effect. To achieve these research objectives, the research methods used were as follows:

A Piper trilinear diagram and saturation index of main mineral components were used to determine the hydrochemical characteristics of geothermal water, carbonated thermal water springs, and groundwater in Xining Basin, and to determine the evolution path from recharge area to geothermal water. The molar concentration ratio of the main ion components in the water was used to analyze the hydrogeochemical process of the formation of the main ions in the carbonated thermal water spring and the mechanism of water-rock interaction. The relationship between $\delta^2\text{H}$ and $\delta^{18}\text{O}$ isotopes was used to determine the recharge source of geothermal water and carbonated thermal water springs in Xining Basin. Geothermal water ^{14}C dating and helium isotope R/Ra values were used to determine whether there may be a fluid (gas) source from the deep mantle in geothermal water. Calcareous uranium series dating was used to determine the formation age of geothermal water. The relationship between the $\delta^{13}\text{C}$ value of CO_2 and the volume fraction of CO_2 in carbonated thermal water springs was used to determine whether the CO_2 was of inorganic origin, biological origin, or both. The $\delta^{13}\text{C}$ range of travertine was used to

analyze whether the cause of travertine was surface travertine or endogenous travertine. The enrichment status of Eu (Europium) and Ce (Cerium) in travertine rare earth elements was used to determine the material source of travertine.

4. Results and Discussion

4.1. Geochemical Characteristics of Water, Gas, and Travertine

(1) Hydrochemical characteristics of geothermal water (containing carbonated thermal water spring) and cold groundwater

The chemical composition of groundwater is the result of chemical reactions between water and minerals in the aquifer under certain temperatures and pressures. In a study of the causes of groundwater and the hydrogeological environment, it is necessary to scientifically classify the chemical composition of water. Piper proposed a trilinear diagram for the classification of water chemical composition in 1944, which was widely used later.

As can be seen from Figure 2, Zone I is the cold groundwater of Yaoshuitan in the front of the Laji Mountain, which is located in the front of the mountain and the thin overlying layer. The main hydrochemical types are $\text{HCO}_3\text{-SO}_4\text{-Ca}\cdot\text{Na}\cdot\text{Mg}$ or $\text{HCO}_3\text{-SO}_4\text{-Ca}\cdot\text{Na}\cdot\text{Mg}$, and the main anions are HCO_3^- and SO_4^{2-} ; the HCO_3^- content is 312–345 mg/L. The mineralization degree is relatively low, 573–590 mg/L, which can represent the recharge area of groundwater in Xining Basin.

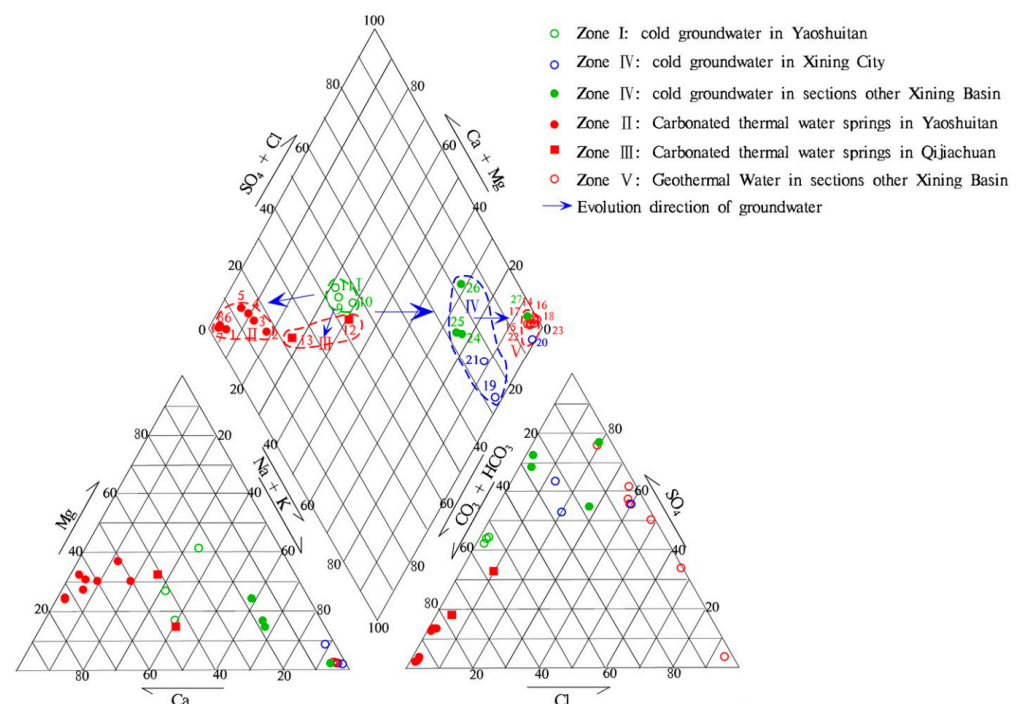


Figure 2. Piper trilinear diagram of geothermal water and cold groundwater in Xining Basin.

Zone II is the Yaoshuitan carbonated thermal water spring, the cations are mainly Ca^{2+} and Mg^{2+} , and the hydrochemical types are mainly $\text{HCO}_3\text{-Ca}\cdot\text{Mg}$ and $\text{HCO}_3\text{-Ca}$ (Table 1). It shows remarkable characteristics of carbonate groundwater, and the salinity of geothermal water is 993–1850 mg/L, which is significantly higher than that of the cold groundwater below Shuitan beach. The main anion is HCO_3^- , and the content of HCO_3^- is 996~1989 mg/L, which is significantly higher than that of cold groundwater in the same area. This could attribute to the mixing of a large amount of CO_2 from deep. The saturation index of soluble anhydrite and gypsum in Yaoshuitan carbonated thermal water spring is obviously higher than that of cold groundwater, and the saturation index of soluble stone salt is lower than that of cold groundwater, and the saturation index of relatively insoluble aragonite, calcite, and dolomite was higher than that of cold groundwater (Table 2 and

Figure 3). This is because the content of anhydrite, gypsum, aragonite, calcite, and dolomite in carbonate reservoir is relatively high, while the content of halite in cold groundwater aquifer of sandstone is relatively high.

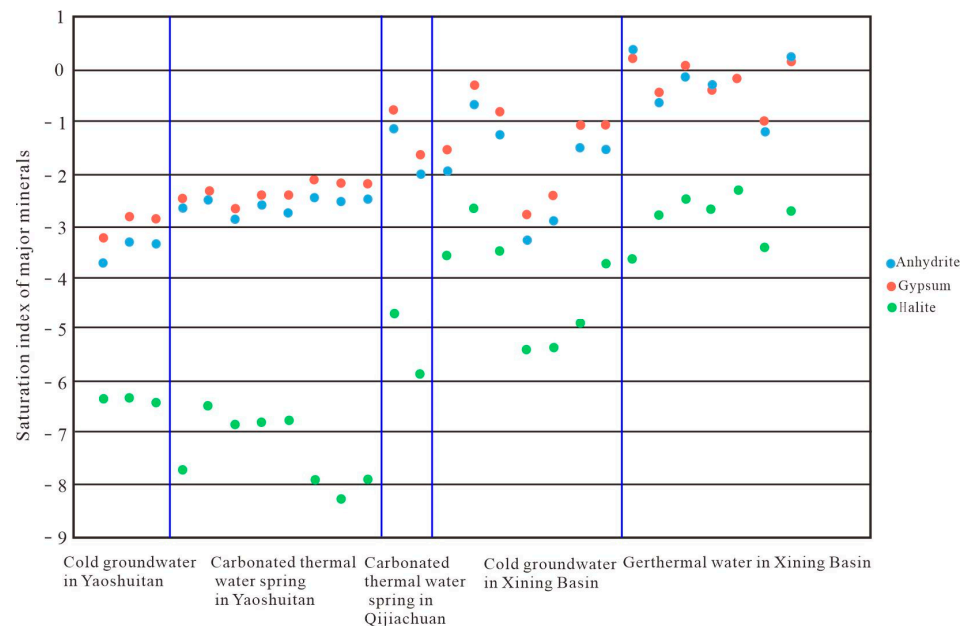


Figure 3. Saturation index distribution of main soluble minerals in carbonated thermal water spring, geothermal water, and cold groundwater in Xining Basin.

Zone III is the carbonated thermal water spring in the Qijiachuan carbonated thermal water spring in Pingan County. The mineralization degree of the Qijiachuan carbonated thermal water spring is 2940~5470 mg/L, which is obviously higher than that of the Yaoshuitan carbonated thermal water spring. The main anion is HCO_3^- , and the content of HCO_3^- is 1820~3145 mg/L, which is obviously higher than that of cold groundwater in Xining Basin. The main hydrochemical types are $\text{HCO}_3\text{-SO}_4\text{-Mg}\cdot\text{Na}\cdot\text{Ca}$ and $\text{HCO}_3\text{-SO}_4\text{-Ca}\cdot\text{Na}$, which are more complex than Yaoshuitan carbonated thermal water spring. The saturation indices of anhydrite, gypsum, aragonite, calcite, dolomite, stone salt, and potassium salt are significantly higher than those of the Yaoshuitan carbonated thermal water spring and cold groundwater (Figure 3). It indicates that the runoff circulation process is relatively sufficient and there is obvious mixing between deep circulating carbonate geothermal water and shallow sandstone groundwater, and the degree of water-rock interaction is higher than that of the Yaoshuitan carbonated thermal water spring. In Figure 2, it is located on the right side of area II, and the location is relatively scattered. This is because the Qijiachuan is relatively far from the groundwater recharge area in the piedmont of the Laji Mountain, and there are thick sandstone and mudstone cap rocks above the carbonate reservoir. There is a phenomenon of frequent mixing of carbonate groundwater and sandstone groundwater.

Zone IV is the cold ground water in other parts of the Xining Basin, which is located in the runoff-discharge zone of shallow groundwater and is to the right on the Piper trilinear diagram (Figure 2). The salinity of groundwater ranges from 265 to 2820 mg/L. The salinity of shallow groundwater is equal to that of the recharge area. The salinity of cold groundwater significantly increases as it goes deeper into the basin. It indicates that, with the increase of water-rock interaction degree, the more soluble components of groundwater dissolved surrounding rock. The main hydrochemical types are $\text{SO}_4\text{-Cl-Na}$ and $\text{SO}_4\text{-HCO}_3\text{-Na}$, which are more complex than the cold groundwater in the recharge area. The saturation indices of anhydrite, gypsum, aragonite, calcite, dolomite, stone salt, and potassium salt are significantly higher than those of the cold groundwater in the recharge area (Figure 3), indicating that the degree of water-rock interaction experienced was relatively high.

Table 1. Test results of main chemical components of carbonated thermal water springs, geothermal water, and groundwater in Xining Basin.

Type	Sample Number	T (°C)	pH	K ⁺ /mg/L	Na ⁺ /mg/L	Ca ²⁺ /mg/L	Mg ²⁺ /mg/L	Cl ⁻ /mg/L	SO ₄ ²⁻ /mg/L	HCO ₃ ⁻ /mg/L	δ ¹⁸ O/VSMOW‰	δ ² H/VSMOW‰	TDS (mg/L)	Hydrochemical Type
Carbonated thermal water spring of Yaoshuitan	1	37	6.68	4.63	20.1	317.4	93.7	7.5	45.4	1310.0			1850	HCO ₃ -Ca
	2	41.5	6.91	2.50	97.5	225.4	83.2	12.7	153.7	1156.9	-10.11	-67.36	1550	HCO ₃ -Ca·Mg
	3	35	7.12	3.81	47.9	196.7	88.1	6.3	129.5	995.9			993.5	HCO ₃ -Ca·Mg
	4	38	7.03	3.75	47.4	285.7	88.4	9.1	153.0	1221.0			1221	HCO ₃ -Ca·Mg
	5	22	7.05	2.36	43.1	394.7	97.1	7.3	176.9	1544.0			1510	HCO ₃ -Ca·Mg
	6 *	18.2	6.45	3.01	13.1	457	94.6	12.9	43.4	1774			1536	HCO ₃ -Ca·Mg
	7 *	21.5	6.12	1.86	9	309	88	12.9	27.1	1291	-9.8	-61	1111	HCO ₃ -Ca·Mg
	8 *	27.3	6.55	3.73	15.6	509	105	10.6	40.1	1989			1707	HCO ₃ -Ca·Mg
Cold groundwater of Yaoshuitan	9	10	7.81	0.76	77.9	49.4	49.5	3.5	228	344.7			589.4	HCO ₃ ·SO ₄ -Mg·Na·Ca
	10	7	7.74	1.13	89	83	20	5.25	206.5	312.3			574.1	HCO ₃ ·SO ₄ -Ca·Na
	11	9	8.02	1.04	70	78.5	32.1	5.25	209.8	330			572.9	HCO ₃ ·SO ₄ -Ca·Na·Mg
carbonated thermal water spring of Qijiachuan	12	21	6.54	0	756.5	739.5	145.4	294.2	1359	3145			5470	HCO ₃ ·SO ₄ -Ca·Na
	13	17	6.63	68.8	189	300.5	145.5	58.2	320	1820	-10.6	-75	2940	HCO ₃ -Ca·Mg·Na
Geothermal water of Pingan	14	67	7.20	80.69	15,100	549.6	176.1	22,600	1220	750			40,600	Cl-Na
Geothermal water of Xining	15	36	7.70	37.1	9352	242.6	116.9	5865	11,321	1427			27,696	SO ₄ ·Cl-Na
	16	34	7.44	42.9	14,460	548.4	139.8	11,729	15,370	524.5			42,604	Cl·SO ₄ -Na
	17	61	7.56	124.0	11,100	270.1	78.3	6980	14,200	1410	-10.4	-74	34,200	SO ₄ ·Cl-Na
	18	53	8.41	48.74	16,600	425.6	140.0	9360	20,700	700	-10.2	-71	48,000	SO ₄ ·Cl-Na
Cold groundwater of Xining	19	—	8.34	18.22	3650	41.36	19.36	1200	4160	2820			12,000	SO ₄ ·Cl-Na
	20	15.2	7.56	73	10,600	293.1	71.9	6860	12,900	1340			32,200	SO ₄ ·Cl-Na
	21	12.7	7.52	15	3092	280.6	63.9	899.7	5773	2720			12,300	SO ₄ ·HCO ₃ -Na
Other geothermal water in Xining Basin	22	34	8.00	17.5	3735	141.2	32	1293	6258	508			11,992	SO ₄ ·Cl-Na
	23	62	7.65	37.3	14,330	567.7	107	15,993	10,726	249.8			41,820	Cl·SO ₄ -Na
Other cold groundwater in Xining Basin	24	7	8.43	0.97	276.6	67.6	29.2	8.75	602	277			1139	SO ₄ ·HCO ₃ -Na
	25	9	7.80	2.96	288	70.6	38.7	19.96	614	335.9			1226	HCO ₃ ·SO ₄ -Na
	26	10	7.53	4.63	539.8	152.2	117.3	385.2	1021	429			2492	SO ₄ ·Cl-Na·Mg
	27	8	7.40	11.4	2312	120.5	18.4	745.5	4114	265.4			7590	SO ₄ -Na

Note: Samples marked with an asterisk are from [28].

Table 2. Saturation index of main minerals in carbonated thermal water spring, geothermal water, and groundwater in Xining Basin.

Type	Sample Number	T (°C)	pH	Anhydrite (CaSO ₄)	Aragonite (CaCO ₃)	Calcite (CaCO ₃)	Dolomite CaMg(CO ₃) ₂	Gypsum (CaSO ₄ ·2H ₂ O)	Halite (NaCl)	Sylvite (KCl)	TDS	Hydrochemical Type
Carbonated thermal water spring of Yaoshuitan	1	37	6.68	−2.65	0.64	0.78	1.50	−2.47	−7.68	−7.93	1850	HCO ₃ -Ca
	2	41.5	6.91	−2.48	0.75	0.88	1.83	−2.35	−6.47	−7.68	1550	HCO ₃ -Ca·Mg
	3	35	7.12	−2.87	0.77	0.91	1.92	−2.67	−6.83	−7.54	993.5	HCO ₃ -Ca·Mg
	4	38	7.03	−2.58	0.93	1.07	2.10	−2.42	−6.78	−7.50	1221	HCO ₃ -Ca·Mg
	5	22	7.05	−2.74	0.94	1.09	1.88	−2.41	−6.76	−7.57	1510	HCO ₃ -Ca·Mg
	6 *	18.2	6.45	−2.48	0.40	0.55	0.68	−2.10	−7.88	−8.05	1536	HCO ₃ -Ca·Mg
	7 *	21.5	6.12	−2.53	−0.14	0.01	−0.21	−2.19	−8.24	−8.47	1111	HCO ₃ -Ca·Mg
	8 *	27.3	6.55	−2.49	0.70	0.84	1.38	−2.21	−7.86	−8.05	1707	HCO ₃ -Ca·Mg
Cold groundwater of Yaoshuitan	9	10	7.81	−3.72	0.14	0.30	0.72	−3.25	−6.32	−7.83	589.4	HCO ₃ ·SO ₄ -Mg·Na-Ca
	10	7	7.74	−3.32	0.22	0.37	0.19	−2.82	−6.30	−7.68	574.1	HCO ₃ ·SO ₄ -Ca·Na
	11	9	8.02	−3.35	0.52	0.67	1.06	−2.87	−6.40	−7.72	572.9	HCO ₃ ·SO ₄ -Ca·Na·Mg
Carbonated thermal water spring of Qijiachuan	12	21	6.54	−1.15	0.81	0.96	1.51	−0.80	−4.69	/	5470	HCO ₃ ·SO ₄ -Ca·Na
	13	17	6.63	−2.03	0.37	0.52	0.97	−1.64	−5.86	−5.83	2940	HCO ₃ -Ca·Mg·Na
Geothermal water of Pingan	14	67	7.20	0.34	0.79	0.91	1.59	0.21	−3.65	−5.74	40,600	Cl-Na
Geothermal water of Xining	15	36	7.70	−0.64	1.05	1.18	2.48	−0.46	−2.80	−4.86	27,696	SO ₄ ·Cl-Na
	16	34	7.44	−0.15	0.62	0.76	1.33	0.04	−2.49	−4.69	42,604	Cl·SO ₄ -Na
	17	61	7.56	−0.33	1.19	1.32	2.51	−0.40	−2.67	−4.38	34,200	SO ₄ ·Cl-Na
	18	53	8.41	−0.19	1.57	1.69	3.36	−0.19	−2.32	−4.60	48,000	SO ₄ ·Cl-Na
Cold groundwater of Xining	19	—	8.34	−1.94	1.09	1.24	2.40	−1.54	−3.56	−5.39	12,000	SO ₄ ·Cl-Na
	20	15.2	7.56	−0.69	0.68	0.83	1.29	−0.30	−2.66	−4.39	32,200	SO ₄ ·Cl-Na
	21	12.7	7.52	−1.25	1.09	1.25	2.03	−0.82	−3.49	−5.32	12,300	SO ₄ ·HCO ₃ -Na
Other geothermal water in Xining Basin	22	34	8.00	−1.19	0.84	0.98	1.74	−0.99	−3.39	−5.34	11,992	SO ₄ ·Cl-Na
	23	62	7.65	0.23	0.74	0.86	1.34	0.14	−2.70	−5.08	41,820	Cl·SO ₄ -Na
Other cold groundwater in Xining Basin	24	7	8.43	−3.28	0.69	0.84	1.39	−2.78	−5.37	−7.30	1139	SO ₄ ·HCO ₃ -Na
	25	9	7.80	−2.91	0.20	0.36	0.55	−2.43	−5.35	−6.83	1226	HCO ₃ ·SO ₄ -Na
	26	10	7.53	−1.52	0.24	0.40	0.81	−1.05	−4.90	−6.47	2492	SO ₄ ·Cl-Na·Mg
	27	8	7.40	−1.55	−0.36	−0.21	−1.13	−1.06	−3.72	−5.53	7590	SO ₄ -Na

Note: Samples marked with an asterisk are from [28].

Zone V is the deep buried sandstone geothermal water in the urban area of Xining City and other parts of Xining Basin. The degree of water-rock interaction is high, which is on the right side of the Piper trilinear diagram (Figure 2). The mineralization degree of geothermal water ranges from 11,992 to 42,604 mg/L, which is obviously higher than that of the Yaoshuitan and Qijiachuan carbonated thermal water springs, and is also higher than that of cold groundwater in the basin. The main hydrochemical types are $\text{SO}_4\text{-Cl-Na}$ and $\text{Cl-SO}_4\text{-Na}$, which are more complex than the cold groundwater and geothermal water in the recharge area at the basin margin. The saturation indices of anhydrite, gypsum, aragonite, calcite, dolomite, stone salt, and potassium salt are significantly higher than those of carbonated thermal water springs in Yaoshuitan and Qijiachuan, and also significantly higher than those of cold groundwater in the basin (Figure 3). It shows that it has experienced a full runoff-cycle process and is in a closed hydrogeological environment inside the deeply buried sedimentary basin with slow runoff.

From the recharge area (Zone I) at the edge of Xining Basin to the cold groundwater area (Zone IV) and geothermal water area (Zone V) in the basin, it reflects the normal evolution path of the basin groundwater from the recharge area to the runoff and discharge area in the basin. From the recharge area of Xining Basin to the interior of the basin, the evolution of groundwater is mainly divided into two branches, one is from the recharge area at the basin edge to the cold groundwater area at the shallow part of the basin, and the other is from the recharge area at the basin edge to the geothermal water area in the deep part of the basin. From the recharge area at the edge of Xining Basin (Zone I) to the carbonated thermal water springs area near the edge of Xining Basin (Zone II and III), it is opposite to the normal evolution path of groundwater in the basin, which is due to the mixing of a large amount of CO_2 gas along the deep fault zone of the northern margin of the Laji Mountain along the edge of the basin. The addition of a large amount of CO_2 not only changes the hydrochemical type of groundwater, but also makes the anions HCO_3^- and SO_4^{2-} , which change to HCO_3^- . It also makes the solubility of carbonated thermal water springs stronger and the degree of mineralization significantly increases. The pH values of carbonated thermal water spring range from 6.12 to 6.91, which is weakly acidic. Therefore, its genesis cannot be a strongly acidic magmatic heat source geothermal system [35].

(2) Water-Rock Interaction and Evolution Process

The ratio of Na^+/Cl^- equal to 1 is usually attributed to salt dissolution. As shown in Figure 4a, the Na^+/Cl^- ratio of the carbonated thermal water spring and its nearby groundwater is much higher than 1. Therefore, there is additional source of Na^+ in addition to halite dissolution. The molar ratio of Na^+/Cl^- in the Qijiachuan carbonated thermal water spring with thick cap rock is higher than that in the Yaoshuitan carbonated thermal water spring, indicating that the deeper the carbonate reservoir is buried, the stronger the dissolution of silicate minerals from deep metamorphic sandstone and slate [36]. In addition, if Ca^{2+} , Mg^{2+} , HCO_3^- , and SO_4^{2-} only come from calcite, dolomite, and gypsum weathering, the molar ratio of $(\text{Ca}^{2+} + \text{Mg}^{2+})$ and $(\text{HCO}_3^- + \text{SO}_4^{2-})$ should be 1. Figure 4b shows that the molar ratio of $(\text{Ca}^{2+} + \text{Mg}^{2+})$ and $(\text{HCO}_3^- + \text{SO}_4^{2-})$ is very close to 1, indicating that the water-rock interaction is dominated by the dissolution of calcite, dolomite, and gypsum in deep carbonate reservoirs. The $\text{HCO}_3^- + \text{SO}_4^{2-}$ value in the Qijiachuan carbonated thermal water spring is greater than the $\text{Ca}^{2+} + \text{Mg}^{2+}$ value, and the excess $\text{HCO}_3^- + \text{SO}_4^{2-}$ must be balanced by Na^+ produced by the dissolution of silicate minerals in metamorphic sandstone and slate. The molar ratio of $(\text{Na}^+ + \text{K}^+)/\text{HCO}_3^-$ in the Yaoshuitan carbonated thermal water spring, groundwater, and the Qijiachuan carbonated thermal water spring is far less than 1 (Figure 4c), and the molar ratio of $(\text{Na}^+ + \text{K}^+)/\text{HCO}_3^-$ in the Qijiachuan carbonated thermal water spring is smaller than in Yaoshuitan. It indicates that the dissolution of silicate minerals plays a minor role in the chemical composition formation of carbonated thermal water springs in Xining Basin. These results indicate that the hydrochemical composition of Yaoshuitan and Qijiachuan carbonated thermal water springs in Xining Basin is likely controlled by the dissolution of calcite, dolomite, and gypsum in deep carbonate reservoirs, supplemented by the dissolution of silicate minerals. The deeper the

burial of carbonate reservoirs, the thicker the sandstone and mudstone cap rocks, and the stronger the effect of dissolution of silicate minerals on chemical composition [37,38].

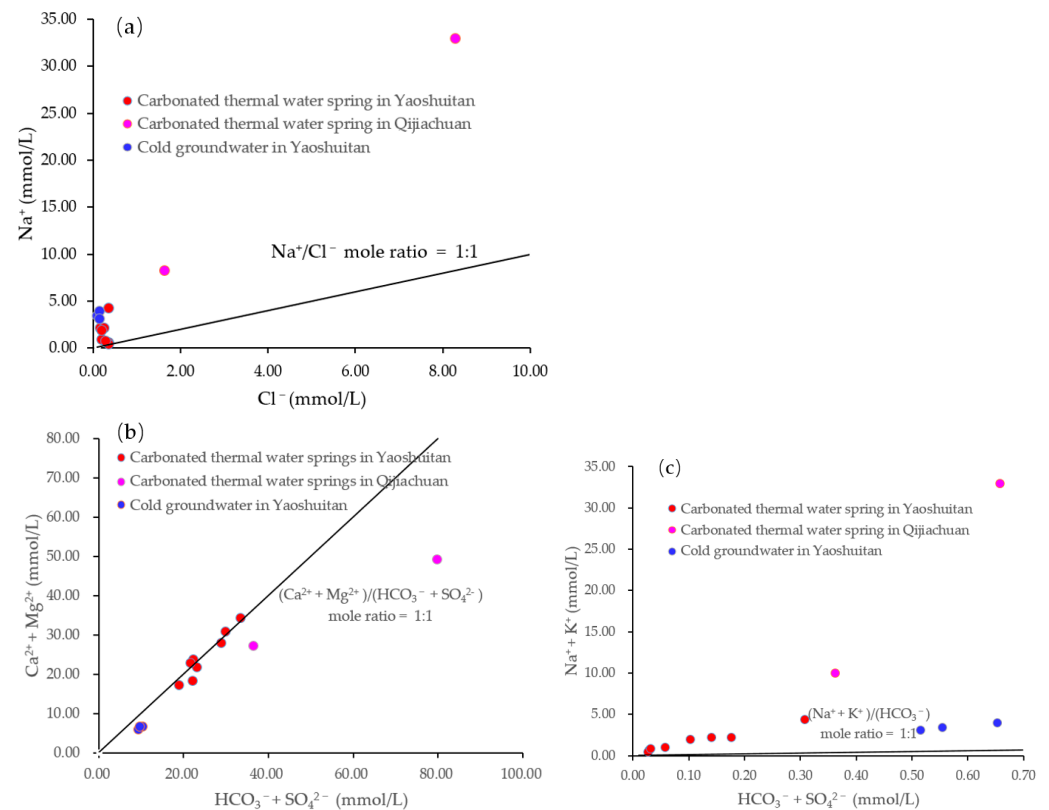


Figure 4. (a) Relationship between Na^+ and Cl^- , (b) relationship between $\text{Ca}^{2+} + \text{Mg}^{2+}$ and $\text{HCO}_3^- + \text{SO}_4^{2-}$, (c) relationship between $\text{Na}^+ + \text{K}^+$ and HCO_3^- for water samples from Yaoshuitan and Qijiachuan.

(3) Gas composition and weak acid origin

The gas sample compositions of the Yaoshuitan and Qijiachuan carbonated thermal water springs show that the gas component in the carbonated thermal water springs is mainly CO_2 , and CO_2 in most sample gasses is about 90%, followed by N_2 and O_2 (Table 3). The CO_2 volume fraction of the Yaoshuitan geothermal field is slightly lower than that of the Qijiachuan geothermal field, which may be due to the thin cover layer of the Yaoshuitan geothermal field, and the more adequate contact between the geothermal water and the atmosphere, thus absorbing more air components. The Qijiachuan geothermal field has thick cap rocks, which isolate the contact between the geothermal water and the air, so the CO_2 volume fraction is high.

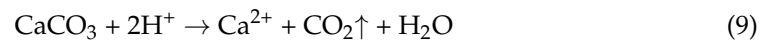
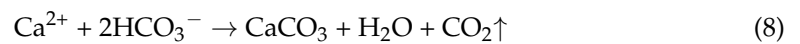
Table 3. Composition and content of gas phases in groundwater studied.

Number	Sampling Location	Gas Sample Composition Data (%)					PDB/ $\delta^{13}\text{C}_{\text{CO}_2}$ Accuracy: $\pm(0.2\sim 0.5)\%$	$^3\text{He}/^4\text{He}$	R/Ra
		CO_2	N_2	O_2	Ar	CH_4			
1 #	Shangraozhuang	90.28	7.45	2.17	0.10	0	-1.94	1.42×10^{-6}	1.01
2 #	Binglingshan 1	93.95	4.59	1.40	0.067	0	-3.27~-2.24	1.02×10^{-6}	0.73
3 #	Binglingshan 2	94.14	4.44	1.35	0.067	0	-2.53	0.62×10^{-6}	0.44
4 #	ZK10 well	87.63	9.66	2.58	0.13	0	-1.46	0.0626×10^{-6}	0.04
5 *	Yaoshuitan 16	64.12	31.03	4.44	0.36	0	—	—	—
6 *	Yaoshuitan 64	88.12	10.36	1.34	0.12	0	—	—	—

Notes: Samples marked with “#” are from [32]; samples marked with “*” are from the internal data of the Qinghai New Energy Research Institute (1986).

There are generally three sources of CO_2 in groundwater: (1) Soil CO_2 produced by the decomposition of organic matter (humus) in the soil or the respiration of plant roots. The $\delta^{13}\text{C}$

Calcite is the main component in carbonated thermal water spring travertine at Qijiachuan, accounting for 66 to 97% [42], and the pores of the travertine are mostly filled with secondary calcite [34], which indicates that the carbonated thermal water spring travertine in the Qijiachuan may be formed in the deep geological environment with a temperature of 150–200 °C. The CO₂ formed during the metamorphism of deep carbonates and silicates under high temperature and pressure migrates along the surface of the Laji Mountain fault zone and its secondary faults or the faults where it intersects, forming weakly acidic carbonated thermal water spring [43]. Weak acidity enhances the solubility of water to carbonate. This carbonated thermal water spring comes into contact with carbonate rock to further generate CO₂ and form calcification at the discharge point. At the same time, because the dissolution reaction of acid water to carbonate rocks consumes H⁺, the acidity of water becomes weak, so the carbonated thermal water spring shows weak acidity, rather than strong acidity. The general reaction is as follows:



(4) Isotopic composition of water

In order to describe the linear relationship between $\delta^2\text{H}$ and $\delta^{18}\text{O}$ stable isotopes in Meteoric Water, Craig published the famous Global Meteoric Water Line (GMWL) equation in 1961 [44]. The Craig line should be widely used as a comparative benchmark in the study of water cycles, especially precipitation processes [45]. As can be seen from Figure 6, geothermal water in the study area falls near the GMWL line, indicating that the main recharge source of geothermal water in the study area is atmospheric precipitation. However, the ^{18}O of the Yaoshuitan carbonated thermal water spring has an obvious negative drift, which is because the geothermal spring contains a large amount of C¹⁶O₂ gas. The ^{16}O in C¹⁶O₂ reacts with the ^{18}O in water by displacement (equilibrium fractionation). The reaction formula is as follows:

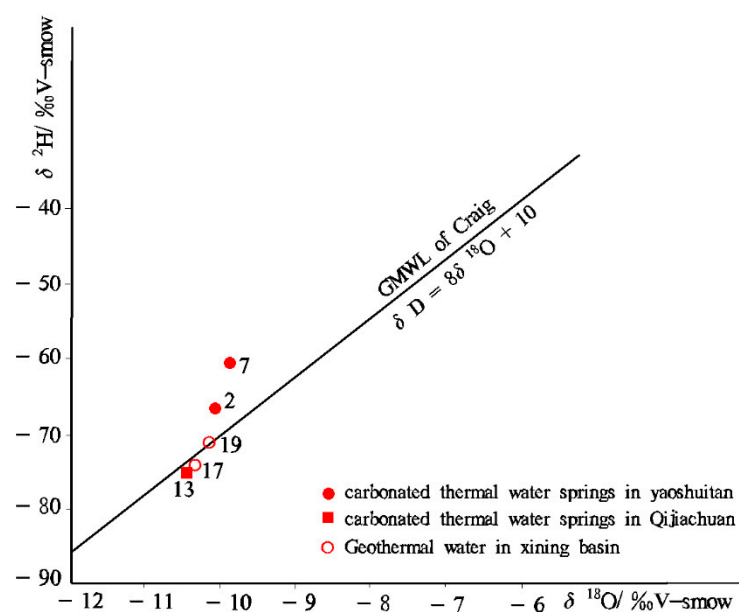
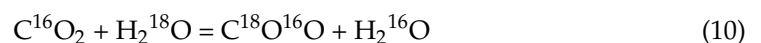


Figure 6. The relationship between $\delta^2\text{H}$ and $\delta^{18}\text{O}$ in the geothermal water of Xining Basin.

Displacement reaction caused ^{18}O in the carbonated thermal water spring to decrease and ^{18}O negative drift occurred [46].

Sun (2015) and Li et al. (2007) conducted ^{14}C dating of geothermal water in the Yaoshuitan and Qijiachuan carbonated thermal water springs, and showed that the ^{14}C age of carbonated thermal water spring was $25.50 \pm 0.50 \sim 47.61 \pm 2.86$ ka [28,47], which was similar to the age of sandstone geothermal water in Xining Basin. The presence of more than 20,000-year-old components in the shallow carbonated thermal water spring in the recharge area indicates that some of these carbonated thermal water spring may come from deep fluid (gas) sources. Fu et al. (2019) conducted uranium-series dating of carbonated thermal water spring travertines at Qijiachuan, showing that the travertine ages approximately range from 16.82 ± 1.38 to 53.768 ± 1.63 ka (Table 4), which is roughly equivalent to the age of local carbonate geothermal water [34].

Table 4. Dating analysis results of travertine uranium series of carbonated thermal water springs in Qijiachuan, Ping'an County (according to [34]).

Number	U ($\mu\text{g/g}$)	Th ($\mu\text{g/g}$)	$\text{U}^{234}/\text{U}^{238}$	$\text{Th}^{230}/\text{Th}^{232}$	Age/ka
1	22.0	0.338	2.37	2.44	24.459 ± 2.17
2	9.42	3.57	1.09	2.10	16.820 ± 1.38
3	19.2	0.23	2.47	1.93	28.306 ± 2.84
4	19.4	0.718	1.53	5.50	23.130 ± 1.96
5	10.9	2.08	1.46	1.48	43.167 ± 5.26
6	28.1	2.37	1.46	0.65	23.973 ± 1.66
7	10.0	3.74	1.01	1.55	53.768 ± 1.63

It can be seen from Table 3 that the R/Ra of the carbonated thermal water spring samples at Qijiachuan is mostly less than 1, indicating that the helium in the geothermal water is mainly of crust-derived helium origin, and there is basically no deep mantle-derived material source.

(5) Travertine characteristics

Pentecost (1995) found that thermogenic travertines mostly occur in areas with strong neotectonic activity, where there is high CO_2 emission [48]. The $\delta^{13}\text{C}$ range of carbonated thermal water spring travertine in Qijiachuang River is $+10.57\text{‰} \sim +11.99\text{‰}$ [49], and the $\delta^{13}\text{C}$ value of endogenous travertine is in the range of $-2\text{‰} \sim +10\text{‰}$ [50], indicating that it is due to the degasification of thermogenic CO_2 .

The content characteristics of rare earth elements in groundwater are usually related to the pH value and redox conditions of the geological environment. The pH value is the most important physical and chemical parameter affecting the content of rare earth elements in geological environments. The chemical properties of Eu (Europium) and Ce (Cerium) in rare earth elements are active, and the reaction to the acidity and alkalinity of geological environment is very obvious, which is prone to fractionation during whole geological process. Under the condition of acidic medium, Eu can easily migrate with the medium, so the content decreases, and Ce is enriched, while under the condition of alkaline medium, the chemical properties of Ce are active, and the content decreases with the migration of the medium, and, at the same time, Eu is enriched [51]. The travertine analysis data from Qijiachuan showed that δEu was significantly less than 1, indicating that Eu was in a state of deficit, and δCe was greater than 1, indicating that Ce was enriched [34]. It indicates that the groundwater providing the source of travertine materials has been under acidic conditions for a long time, which is supplied by CO_2 from deep in the Earth's crust. This kind of groundwater was degassed and deposited to form travertine when it reached the surface. This slightly acidic environment ensures the continuous reaction of carbonated thermal water springs and carbonate rocks, as well as the continuous generation of CO_2 , resulting in the release of a large amount of CO_2 from surface discharge outlets.

4.2. Genesis of Carbonated Thermal Water Spring and Geothermal Significance

The $\delta^2\text{H}$ and $\delta^{18}\text{O}$ isotopic characteristics indicate that the recharge source of carbonated thermal water springs in Xining Basin is mainly atmospheric precipitation. The ^{14}C ages of carbonated thermal water springs are $25.50 \pm 0.50\sim 47.61 \pm 2.86$ ka, indicating that some of these carbonated thermal water springs may be derived from deep fluid (gas) sources. The R/R_a in the carbonic acid geothermal spring is mostly less than 1, indicating that the helium in the geothermal water is mainly caused by crust-derived helium, and there is basically no deep mantle-derived material source.

The Piper trilinear diagram shows that from the recharge area at the edge of Xining Basin to the Yaoshuitan and Qijiachuan carbonated thermal water spring areas, the direction of the normal groundwater evolution path of the basin is contrary to that of the basin, which is due to the large amount of CO_2 gas mixed in the deep fault along the northern margin of Laji Mountain. The ratio of $(\text{Ca}^{2+} + \text{Mg}^{2+})$ and $(\text{HCO}_3^- + \text{SO}_4^{2-})$ in the Yaoshuitan carbonated thermal water spring is close to 1, indicating that the water-rock interaction is dominated by the dissolution of calcite, dolomite, and gypsum in deep carbonate reservoir. The molar concentration of $\text{HCO}_3^- + \text{SO}_4^{2-}$ in the Qijiachuan carbonated thermal water spring is significantly higher than that of $\text{Ca}^{2+} + \text{Mg}^{2+}$. The molar ratio of $(\text{Na}^+ + \text{K}^+)/\text{HCO}_3^-$ in the Yaoshuitan carbonated thermal water spring, groundwater, and the Qijiachuan carbonated thermal water spring is far less than 1. It is indicated that the hydrochemical composition of the Yaoshuitan and Qijiachuan carbonated thermal water springs in Xining Basin is likely controlled by the dissolution of calcite, dolomite, and gypsum in deep carbonate reservoirs, supplemented by the dissolution of silicate minerals. The $\delta^{13}\text{C}$ value of the Qijiachuan carbonated thermal water spring is $-3.27\sim -1.46\%$. The relationship between CO_2 volume fraction and $\delta^{13}\text{C}$ value (PDB) of carbon isotopes of CO_2 indicates that the CO_2 source is of inorganic origin, which is mainly formed by metamorphic decomposition of deep carbonate and marble. Calcite is the main component of carbonated thermal water spring travertine, indicating that the reaction temperature is mainly $150\sim 200$ °C. The $\delta\text{Eu} < 1$ and $\delta\text{Ce} > 1$ in the calcium center of carbonated thermal water springs indicate that the groundwater supplying the travertine material has been in the acidic environment receiving the CO_2 supply from the deep crust for a long time. The groundwater reaches the surface and degasses and deposits to form travertine.

The CO_2 formed during the metamorphism of deep carbonate and silicate under high temperature and high pressure migrates along the Lajishan fault zone and its secondary faults or the surface of the faults that intersect with it, forming weak acid carbonated thermal water springs. Acidity enhances the solubility of water to carbonate rocks, and this carbonated thermal water spring comes into contact with carbonate rock to further generate CO_2 . At the same time, due to the dissolution reaction of acidic water to carbonate rocks, H^+ is consumed, which weakens the acidity of water and makes carbonated thermal water springs weakly acidic.

The genetic mechanism of the carbonated thermal water springs at Yaoshuitan and Qijiachuan in Xining Basin can be summarized as follows: A series of tectonic activities, such as the late collision and post-collision between India and the Eurasian plate, led to the uplift of the northern Qinghai–Tibet Plateau and the asthenosphere upwelling, thermal intrusion, and other deep dynamic processes, which kept a higher thermal background in the eastern Qinghai Province, including Xining Basin. The heat source of carbonated thermal water springs comes from the lower crust and upper mantle. The deep faults on the northern margin of Laji Mountain with obvious neotectonic activity and other deep and large faults provide channels for the intrusion of deep crust–mantle thermal materials, and local geothermal anomalies are formed near the deep and large faults. Concealed carbonate rocks and silicate rocks with greater thicknesses provide the material basis for CO_2 generation. Carbonates and silicates undergo thermal metamorphism under the high-temperature and high-pressure environment in the deep geothermal anomaly to form a large amount of CO_2 . CO_2 dissolved in water enhances the acidity of water, it migrates to the surface along the Laji Mountain fault zone and its secondary faults or the faults

offers good exploratory potential of geothermal resources near the deep and large fault at the edge of Xining Basin.

5. Conclusions

- (1) The $\delta^2\text{H}$ and $\delta^{18}\text{O}$ isotopic characteristics indicate that the recharge source of carbonated thermal water springs in Xining Basin is mainly atmospheric precipitation. The ^{14}C age of carbonated thermal water springs is more than 20 ka, indicating that some of these carbonated thermal water springs may come from deep fluid (gas) sources. The R/R_a in the carbonated thermal water spring is mostly less than 1, indicating that the helium in the geothermal water is mainly caused by crust-derived helium, and there is basically no deep mantle-derived material source.
- (2) The Piper trilinear diagram shows that from the recharge area at the edge of Xining Basin to the Yaoshuitan and Qijiachuan carbonated thermal water spring areas, the direction of the normal groundwater evolution path of the basin is contrary to that of the basin, which is due to the large amount of CO_2 gas mixed in the deep fault along the northern margin of Laji Mountain. The ratios of $(\text{Ca}^{2+} + \text{Mg}^{2+})$ and $(\text{HCO}_3^- + \text{SO}_4^{2-})$ and $f(\text{Na}^+ + \text{K}^+)/\text{HCO}_3^-$ in the Yaoshuitan and Qijiachuan carbonated thermal water springs indicate that the hydrochemical composition of the Yaoshuitan and Qijiachuan carbonated thermal water springs in Xining Basin is controlled by the dissolution of calcite, dolomite, and gypsum in deep carbonate reservoirs, supplemented by the dissolution of silicate minerals. The relationship between CO_2 volume fraction and $\delta^{13}\text{C}$ value (PDB) of carbon isotopes of CO_2 indicates that the CO_2 source is of inorganic origin, which is mainly formed by metamorphic decomposition of deep carbonate and marble. The $\delta\text{Eu} < 1$ and $\delta\text{Ce} > 1$ in the calcium center of carbonated thermal water springs indicate that the groundwater supplying the travertine material has been in the acidic environment receiving the CO_2 supply from the deep crust for a long time.
- (3) A series of tectonic activities, such as late collision and post-collision between the Indian and Eurasian plates, led to the uplift, asthenosphere upwelling, and thermal invasion of the northern Tibetan Plateau and other deep dynamic processes. The deep faults in the northern margin of the Laji Mountain and other deep faults with obvious neotectonic activity provided channels for the up-invasion of deep thermal materials, and local geothermal anomalies were formed near the deep faults. The hidden carbonate rocks and silicate rocks with large thickness undergo thermal metamorphism under high temperature and high pressure in the deep geothermal anomaly area and form a large amount of CO_2 , which is dissolved in water and enhances the acidity of water. At the same time, the dissolution reaction of acidic water to carbonate rocks consumes H^+ , which keeps the carbonated thermal water springs weakly acidic.
- (4) The composition of travertine in carbonated thermal water springs is dominated by calcite, indicating that travertine may be formed in a deep geological environment with a temperature of 150~200 °C, indicating that there are abnormal heat sources in shallow carbonate strata with a burial depth of 3000~4000 m. The abnormal heat source may be caused by the deep fault in the northern margin of Laji Mountain and other deep and large faults channeled the deep crust and mantle heat source, indicating that the deep fault in the northern margin of Laji Mountain has an obvious heat-controlling effect, and there is a good prospect of geothermal resources exploration near the fault.

Author Contributions: Writing—original draft preparation, Y.L. (Yude Lei), Z.Z. and B.Z.; Conceptualization, writing, review and editing, B.Z.; thesis writing instructor, G.W.; English writing and drawing of the paper, J.G.; field investigation, X.T. and D.Z.; field investigation and sampling, Y.L. (Yude Lei), Z.Z. and Y.L. (Yinfei Luo). All authors have read and agreed to the published version of the manuscript.

Funding: This work was jointly funded by the Applied Basic Research Project of Qinghai Provincial Department of Science and Technology (2019-ZJ-7062), Self-funded Science and Technology Project of Qinghai 906 Engineering Investigation and Design Institute (2021-KJ-002), and China Geological Survey Project (DD20189114 and DD20190132).

Data Availability Statement: The raw data supporting the conclusions of this article will be made available by the authors, without undue reservation.

Conflicts of Interest: The authors declare no conflict of interest.

References

1. Du, L. Outgassing of the earth is a key link for the framework of the whole earth science. *Earth Sci. Front.* **2000**, *2*, 381–390. [[CrossRef](#)]
2. Shao, J.; Zhao, Y.; Zhang, F.; Lu, Y. Discussions on Earth degassing and seismic activities in central west Heilongjiang Province. *Acta Petrol. Sin.* **2010**, *26*, 3651–3656.
3. Ostad-Ali-Askari, K. Management of risks substances and sustainable development. *Appl. Water Sci.* **2022**, *12*, 65. [[CrossRef](#)]
4. De Paolo, D.J. Sustainable carbon emissions: The geologic perspective. *MRS Energy Sustain.* **2015**, *2*, E9. [[CrossRef](#)]
5. Orcutt, B.N.; Daniel, I.; Dasgupta, R.; Crist, D.T.; Edmonds, M. 1—Introduction to Deep Carbon: Past to Present. In *Deep Carbon*; Cambridge University Press: Cambridge, UK, 2019; pp. 1–3.
6. Javadinejad, S.; Eslamian, S.; Ostad-Ali-Askari, K. Investigation of monthly and seasonal changes of methane gas with respect to climate change using satellite data. *Appl. Water Sci.* **2019**, *9*, 1–8. [[CrossRef](#)]
7. Bekaert, D.V.; Turner, S.J.; Broadley, M.W.; Barnes, J.D.; Halldórsson, S.A.; Labidi, J.; Wade, J.; Walowski, K.J.; Barry, P.H. Subductiondriven volatile recycling: A global mass balance. *Annu. Rev. Earth Planet. Sci.* **2021**, *49*, 37–70. [[CrossRef](#)]
8. Cheng, Z.; Guo, Z.; Zhang, M.; Zhang, L. Carbon dioxide emissions from Tengchong Cenozoic volcanic field, Yunnan Province, SW China. *Acta Petrol. Sin.* **2014**, *30*, 3657–3670.
9. Zhang, L.; Guo, Z.; Sano, Y.; Zhang, M.; Sun, Y.; Cheng, Z.; Yang, T. Flux and genesis of CO₂ degassing from volcanic-geothermal fields of Gulu-Yadong rift (GYR) in the Lhasa terrane, South Tibet: Constraints on characteristics of deep carbon cycle in the India-Asia continent subduction zone. *J. Asian Earth Sci.* **2017**, *149*, 110–123. [[CrossRef](#)]
10. Xu, S.; Guan, L.; Zhang, M.; Zhong, J.; Liu, W.; Xie, X.; Liu, C.; Takahata, N.; Sano, Y. Degassing of deep-sourced CO₂ from Xianshuihe-Anninghe fault zones in the eastern Tibetan Plateau. *Sci. China Earth Sci.* **2022**, *65*, 139–155. [[CrossRef](#)]
11. Shangguan, Z. A study on deep-seated CO₂ discharge for earthquake prediction. *Seismol. Geol.* **1995**, *17*, 214–217.
12. Barnes, I.; Irwin, W.P.; White, D.E. *Global Distribution of Carbon Dioxide Discharges and Major Zones of Seismicity*; U.S. Geological Survey: Seattle, WA, USA, 1978. [[CrossRef](#)]
13. Chris, M.G.; Crossey, L.J.; Karlstrom, K.E.; Tanner, G. Carbonic springs as distal manifestations of geothermal systems, highlighting the importance of fault pathways and hydrochemical mixing: Example from the Jemez Mountains, New Mexico. *Appl. Geochem.* **2018**, *98*, 45–57. [[CrossRef](#)]
14. Nisi, B.; Vaselli, O.; Elio, J.; Giannini, L.; Tassi, F.; Guidi, M.; Darrah, T.H.; Maletic, E.L.; Huertas, A.; Marchionni, S. The Campo de Calatrava Volcanic Field (central Spain): Fluid geochemistry in a CO₂-rich area. *Appl. Geochem.* **2019**, *102*, 153–170. [[CrossRef](#)]
15. Italiano, F.; Kis, B.M.; Baciu, C.; Ionescuc, A.; Harangib, S.; Palcsud, L. Geochemistry of dissolved gases from the Eastern Carpathians—Transylvanian Basin boundary. *Chem. Geol.* **2017**, *469*, 117–128. [[CrossRef](#)]
16. Shvartsev, S.L.; Kharitonova, N.A.; Lepokurova, O.E.; Chelnokov, G.A. Genesis and evolution of high-pCO₂ groundwaters of the Mukhen spa (Russian Far East). *Russ. Geol. Geophys.* **2017**, *58*, 37–46. [[CrossRef](#)]
17. Kharaka, Y.K.; Abedini, A.A.; Gans, K.D.; Thordson, J.J.; Beers, S.R.; Thomas, R.B. Changes in the chemistry of groundwater reacted with CO₂: Comparison of results from laboratory experiments and the ZERT field site, Bozeman, Montana, USA. *Appl. Geochem.* **2018**, *98*, 75–81. [[CrossRef](#)]
18. Zhang, W.; Wang, Y.; Sun, Z. A Study of the CO₂ genesis of the carbonated hot springs in Hengjing, southern Jiangxi. *Hydrogeol. Eng. Geol.* **2005**, *32*, 6–9. [[CrossRef](#)]
19. Li, J.; Wang, Z.; Wang, Y.; Qiu, X.; Zhang, K.; Li, J. The chemical characteristics and formation mechanisms of carbonate springs along Heyuan fault zone, Guangdong Province. *Zhongshan Daxue Xuebao/Acta Sci. Natralium Univ. Sunyatseni* **2018**, *57*, 19–28. [[CrossRef](#)]
20. Zhou, X.; Wang, W.; Li, I.; Hou, J.; Xing, L.; Li, Z.; Shi, H.; Yan, Y. Geochemical features of hot spring gases in the Jinshajiang-Red River fault zone, Southeast Tibetan Plateau. *Acta Petrol. Sin.* **2020**, *36*, 2197–2214. [[CrossRef](#)]
21. Yu, X.; Wei, Z.; Wang, G.; Ma, X.; Ma, X.; Zhang, T.; Yang, H.; Li, L.; Zhou, S.; Wang, X. Hot Spring Gas Geochemical Characteristics and Geological Implications of the Northern Yadong-Gulu Rift in the Tibetan Plateau. *Front. Earth Sci.* **2022**, *10*, 863559. [[CrossRef](#)]
22. Walter, D.; Li, V.; Lisa, G.; Sergio, C.; Konstantinos, K.; Kyriaki, D. CO₂ release to the atmosphere from thermal springs of Sperchios Basin and northern Euboea (Greece): The contribution of “hidden” degassing. *Appl. Geochem.* **2020**, *119*, 104660. [[CrossRef](#)]
23. Wang, M.; Zhou, X.; Wang, J.; Li, X.; Liu, H. Occurrence, genesis and travertine deposition of the Adong hot springs in northwestern Yunnan of China. *Geothermics* **2020**, *87*, 101851. [[CrossRef](#)]

24. Ta, M.; Zhou, X.; Guo, J.; Wang, X.; Wang, Y.; Xu, Y. The Evolution and Sources of Major Ions in Hot Springs in the Triassic Carbonates of Chongqing, China. *Water* **2020**, *12*, 1194. [[CrossRef](#)]
25. Shi, W.; Zhang, S. Distribution characteristics of geothermal water on the northwestern margin of the Xining basin. *Geol. China* **2006**, *33*, 1131–1136. [[CrossRef](#)]
26. Zhang, S.; Xu, W.; Yan, W.; Wang, J.; Li, Q.; Shi, W. *Xining Basin Geothermal Geology*; Geological Publishing House: Beijing, China, 2013. (In Chinese)
27. Zhao, Z.; Yu, P.; Chen, H.; Luo, Y.; Zhao, D.; Bian, J. Genetic analysis and resource evaluation of the Xining geothermal field in Qinghai Province. *Geol. China* **2015**, *42*, 803–810. [[CrossRef](#)]
28. Li, H.; Zhang, S.; Bai, J.; Zhou, J.; Zhao, Y. Hydrochemistry and Origin of the Yaoshuitan Geothermal Field, Xining, Qinghai. *Acta Geol. Sin.* **2007**, *81*, 1299–1304. [[CrossRef](#)]
29. Sun, H.; Wang, G.; Lin, W. Distribution characteristics and enrichment mechanism of TDS geothermal water in Xining Basin. *Bull. Geol. Sci. Technol.* **2022**, *41*, 278–287. [[CrossRef](#)]
30. Zhang, S.; Li, C.; Sun, W.; Xu, W.; Xin, Y.; Shi, W.; Wang, Z. Construction of the conceptual model of thermal reservoir structure of the Xining Basin, China. *Geol. Bull. China* **2008**, *27*, 126–136. [[CrossRef](#)]
31. Ai, X. Study on CO₂ reservoir and risk zoning evaluation of the tunnel in Xining-Minhe Basin, Qinghai. *Miner. Resour. Geol.* **2021**, *35*, 154–162. [[CrossRef](#)]
32. Zheng, C.; Zhang, H.; Shi, Y.; Hu, L.; Zhang, C. Study on Carbon Dioxide Gas Reservoir Accumulation Mode in Ping'an Region, Qinghai Province. *Northwestern Geol.* **2016**, *49*, 148–154. [[CrossRef](#)]
33. Guo, L.; Wang, G.; Sheng, Y.; Sun, X.; Shi, Z.; Xu, Q.; Mu, W. Temperature governs the distribution of hot spring microbial community in three hydrothermal fields, Eastern Tibetan Plateau Geothermal Belt, Western China. *Sci. Total Environ.* **2020**, *720*, 137574. [[CrossRef](#)]
34. Fu, L.; Zhang, S.; Jia, X.; Li, S.; Yang, T. Test of the paleoenvironment reconstruction of Bingling Hill travertine in large time scale. *Quat. Sci.* **2019**, *39*, 510–517. [[CrossRef](#)]
35. Guo, Q. Magma-heated geothermal systems and hydrogeochemical evidence of their occurrence. *Acta Geol. Sin.* **2020**, *94*, 3544–3554. [[CrossRef](#)]
36. Meybeck, M. Global chemical weathering of surficial rocks estimated from river dissolved loads. *Am. J. Sci.* **1987**, *287*, 401–428. [[CrossRef](#)]
37. Helgeson, H.C.; Garrels, R.M.; MacKenzie, F.T. Evaluation of irreversible reactions in geochemical processes involving minerals and aqueous solutions—II. Applications. *Geochim. Cosmochim. Acta* **1969**, *33*, 455–481. [[CrossRef](#)]
38. Shvartsev, S.L.; Sun, Z.; Borzenko, S.V.; Gao, B.; Tokarenko, O.G.; Zippa, E.V. Geochemistry of the thermal waters in Jiangxi Province, China. *Appl. Geochem.* **2018**, *96*, 113–130. [[CrossRef](#)]
39. Liu, Z.H.; Wolfgang, D. *Karstification Dynamics and Environment*; Geological Publishing House: Beijing, China, 2007. (In Chinese)
40. Muffler, L.; White, D.E. Active Metamorphism of Upper Cenozoic Sediments in the Salton Sea Geothermal Field and the Salton Trough, Southeastern California. *Geol. Soc. Am. Bull.* **1969**, *80*, 157–182. [[CrossRef](#)]
41. Dai, J.; Song, Y.; Dai, C.; Wang, D. Geochemistry and accumulation of carbon dioxide gases in China. *AAPG Bull.* **1996**, *80*, 1615–1626. [[CrossRef](#)]
42. Zhao, Z. Sedimentation and Diagenesis of Binglingshan Travertine. Master's Thesis, Chang'an University, Xi'an, China, 2006.
43. Yan, J.; Zhai, Y.; He, C. Geological characteristics and development and application of natural carbon dioxide gas reservoirs in China. *Geol. Chem. Miner.* **1988**, *2*, 82–91.
44. Craig, H. Isotopic variations in meteoric waters. *Science* **1961**, *133*, 1702–1703. [[CrossRef](#)]
45. Clark, I.D.; Peter, F. *Environmental Isotopes in Hydrogeology*; Lewis Publishers: New York, NY, USA, 1999; pp. 50–98.
46. Dong, H.; Chen, J.; Chen, L. Cause analysis and application of δD and $\delta^{18}O$ drift in water-rock interaction. In *The Chinese Geophysics, 2003-Proceedings of the 19th Annual Meeting of the Chinese Geophysical Society*; Nanjing Normal University Press: Nanjing, China, 2003; pp. 662–663.
47. Sun, K. The Underground Hot Water Circulation Mechanism and Resource Evaluation in Xining Basin. Master's Thesis, Northwestern University, Xi'an, China, 2015.
48. Pentecost, A. The Quaternary travertine deposits of Europe and Asia Minor. *Quat. Sci. Rev.* **1995**, *14*, 1005–1028. [[CrossRef](#)]
49. Du, B. Process of Deposition and Climate Environment Information of Tufa at Binglingshan Qinghai. Master's Thesis, Chang'an University, Xi'an, China, 2006.
50. Liu, Z. Research progress in paleoclimatic interpretations of tufa and travertine. *Chin. Sci. Bull. (Chin. Ver.)* **2014**, *59*, 2229–2239. [[CrossRef](#)]
51. Henderson, P. *Rare Earth Element Geochemistry*; Elsevier: Amsterdam, The Netherlands, 1984.